BIOCHEMISTRY
including biophysical chemistry & molecular biology

Article

pubs.acs.org/biochemistry

Interactions outside the Boundaries of the Canonical Binding Groove of a PDZ Domain Influence Ligand Binding

Celestine N. Chi,[†] S. Raza Haq,[†] Serena Rinaldo,[‡] Jakob Dogan,[†] Francesca Cutruzzolà,[‡] Åke Engström,[†] Stefano Gianni,[§] Patrik Lundström,*[,∥] and Per Jemth*[,†]

[†]Department of Medical Biochemistry and Microbiology, Uppsala University, BMC Box 582, SE-75123 Uppsala, Sweden

[‡]Istituto Pasteur-Fondazione Cenci Bolognetti, Dipartimento di Scienze Biochimiche "A. Rossi Fanelli", Sapienza Università di Roma, Piazzale A. Moro 5, 00185 Rome, Italy

[§]Istituto Pasteur-Fondazione Cenci Bolognetti and Istituto di Biologia e Patologia Molecolari del CNR, Dipartimento di Scienze Biochimiche "A. Rossi Fanelli", Sapienza Università di Roma, Piazzale A. Moro 5, 00185 Rome, Italy

[∥]Division of Molecular Biotechnology, Department of Physics, Chemistry and Biology, Linköping University, SE-58183 Linköping, Sweden

ABSTRACT: The postsynaptic density protein-95/discs large/zonula occludens-1 (PDZ) domain is a protein−protein interaction module with a shallow binding groove where protein ligands bind. However, interactions that are not part of this canonical binding groove are likely to modulate peptide binding. We have investigated such interactions beyond the binding groove for PDZ3 from PSD-95 and a peptide derived from the C-terminus of the natural ligand CRIPT. We found via nuclear magnetic resonance experiments that up to eight residues of the peptide ligand interact with the PDZ domain, showing that the interaction surface extends far outside of the binding groove as defined by the crystal structure. PDZ3 contains an extra structural element, a C-terminal helix (α3), which is known to affect affinity. Deletion of this helix resulted in the loss of several intermolecular nuclear Overhauser enhancements from peptide residues outside of the binding pocket, suggesting that α3 forms part of the extra binding surface in wild-type PDZ3. Site-directed mutagenesis, isothermal titration calorimetry, and fluorescence intensity experiments confirmed the importance of both α3 and the N-terminal part of the peptide for the affinity. Our data suggest a general mechanism in which different binding surfaces outside of the PDZ binding groove could provide sites for specific interactions.

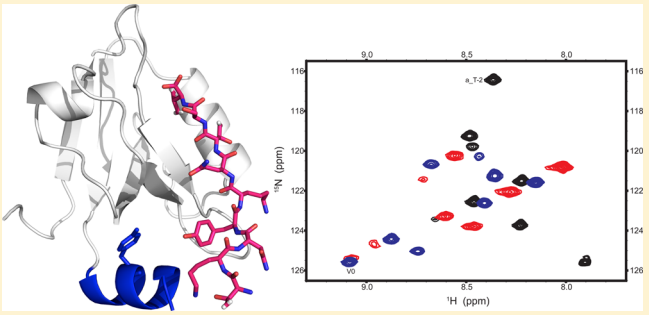

Postsynaptic density protein-95/discs large/zonula occludens-1 (PDZ) domains are usually part of multidomain proteins and coordinate signaling and scaffolding by binding and organizing various cellular proteins.[1−5] They generally bind to short C-terminal sequences in a well-defined binding groove.[6] There are multiple PDZ domains within the same cell and most likely several competing protein ligands present within the vicinity of each PDZ domain. In crystal or nuclear magnetic resonance (NMR) structures of PDZ domains and peptide ligands, usually only four or five ligand residues are visible. Thus, to achieve selectivity toward ligands in a cellular context, factors other than the interactions in the binding groove are likely to play a role. Compartmentalization, local concentration,[7,8] and allosteric effects[9,10] have been proposed as means by which PDZ domains modulate selectivity toward their binding partners.

However, structural elements located outside of the canonical PDZ fold may also influence affinity and specificity. For example, the src homology 3 (SH3) domain modulates the affinity of the adjacent MAGI1 PDZ3.[11,12] Another example is the third PDZ domain of PSD-95 (PDZ3), which contains an α helix located at the C-terminus outside of the canonical PDZ fold[13] (Figure 1). This helix is termed α3, and it curls toward the ligand-binding groove between α2 and β2 of PSD-95 PDZ3. Helix α3 is, however, located more than 5 Å from the last residue that is visible in the crystal structure (Gln_{-3}) of the complex between PDZ3 and the peptide ligand.[13] α3 thus appears not to interact with the ligand. Nevertheless, deletion of helix α3 has a profound effect on the affinity between PDZ3 and peptide ligand, and this helix was suggested to regulate a hidden allostery.[14] Although the peptide ligand residue Tyr_{-5} is not visible in the crystal structure of PDZ3, it contributes to the affinity because its deletion results in a 24-fold decrease in affinity as measured by isothermal titration calorimetry (ITC).[15] It is possible that Tyr_{-5} interacts transiently with PDZ3, via helix α3 or other parts of the PDZ domain. The presence of such very short-lived interactions may have

Received: June 14, 2012
Revised: September 17, 2012
Published: October 9, 2012

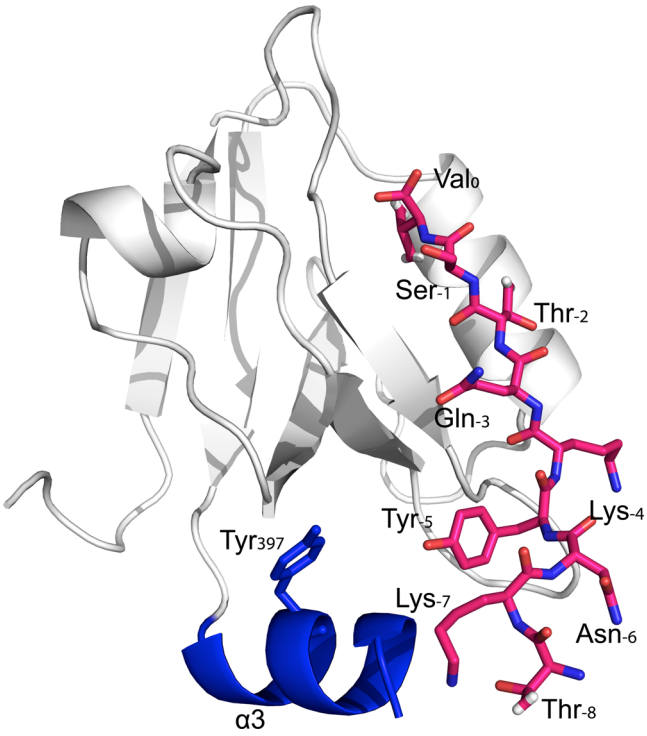

Figure 1. Structure of PDZ3 in complex with a peptide ligand, TKNYKQTSV, adapted from ref 24. Helix α3 and the Tyr_{397} side chain are colored blue. The peptide residues are colored purple and the amide nitrogens blue. The numbering of peptide ligand residues follows the usual convention, starting from 0 at the C-terminus and then −1, −2, etc. This is one of several structures from a molecular dynamics simulation[24] and not a representative average structure. However, it suggests that both Tyr_{397} and Phe_{400} may form transient interactions with Tyr_{-5} of the peptide ligand. The figure was drawn with PyMOL (The PyMOL Molecular Graphics System, DeLano Scientific, LLC).

implications for the whole family of PDZ domains and their interactions with protein ligands.

To test this hypothesis and learn more about interactions outside of the binding groove of PDZ domains, we investigated the role of peptide residues outside of the binding pocket as well as helix α3 in PDZ3 by protein engineering in conjunction with NMR, ITC, and kinetic experiments based on fluorescence. We demonstrate that binding is indeed modulated by interactions beyond the canonical binding groove.

MATERIALS AND METHODS

Expression and Purification of PDZ Variants. The PDZ domain used in this study was PDZ3 from human PSD-95, and it contains the F337W mutation (this construct is hereafter termed PDZ3). The numbering of residues refers to full-length PSD-95α without exon b and is the same as that used by Doyle et al.[13] The F337W mutation serves as a fluorescence probe in ligand binding experiments and does not affect the affinity of the PDZ3−peptide interaction.[16−18] It also does not affect the energetic coupling pattern between side chain residues in the PDZ domain and the peptide ligand,[9] because the coupling energy for F337W is zero with regard to a second mutation in the peptide ligand, either at the C-terminal Val_0 or at Ser_{-2} (not shown). The sequence corresponding to helix α3 (residues 396−401) was deleted from the cDNA of PDZ3 to generate the α3 helix-deleted mutant PDZ3Δα3. The point mutants Y397E, R399A, and F400A in helix α3 were created by inverted polymerase chain reaction on the cDNA encoding PDZ3, using Pfu Turbo polymerase (Stratagene).

Transformed *Escherichia coli* BL21 DE3 pLysS cells were selected by being grown in 2TY medium containing ampicillin (50 μg/mL) and chloramphenicol (35 μg/mL) at 37°C until the OD_{600} reached 0.4−0.6. Protein expression was induced by adding 1 mM isopropyl β-D-thiogalactopyranoside, and the cells were allowed to express protein overnight at 30 °C. The cells were collected by centrifugation (7000*g* for 10 min) and resuspended in buffer [50 mM Tris-HCl (pH 8.5) and 400 mM NaCl]. The cells were then disrupted by ultrasonication, followed by centrifugation (35000*g*) for 1 h. The supernatant thus obtained was filtered successively through 0.45 and 0.2 μm filters (Sarstedt). The filtered supernatant was loaded onto a nickel(II)-charged chelating Sepharose FF column (GE Healthcare), equilibrated with 50 mM Tris-HCl (pH 8.5) and 400 mM NaCl, and washed with 300 mL of the same buffer. The bound protein was eluted with 250 mM imidazole (pH 7.9). The fractions containing the PDZ were pooled, concentrated, and dialyzed overnight against 50 mM Tris-HCl (pH 8.5). The dialyzed protein samples were filtered through 0.2 μm filters and loaded onto a Q-column (GE Healthcare), equilibrated with 50 mM Tris-HCl (pH 8.5). The protein did not bind to the column and appears in the unbound fraction. The fraction containing the protein was run on an S-column (GE Healthcare), equilibrated with 50 mM Tris-HCl (pH 8.5). The bound protein was eluted with a gradient from 0 to 1 M NaCl in 50 mM Tris-HCl (pH 8.5). The fractions containing the PDZ were pooled; the purity of the PDZ variants were checked by sodium dodecyl sulfate−polyacrylamide gel electrophoresis stained with Coomassie brilliant blue, and the identities of the mutants were confirmed by matrix-assisted laser desorption ionization time-of-flight (MALDI-TOF) mass spectrometry. Purified mutants were analyzed by urea denaturation experiments. We observed the typical sigmoidal denaturation curve for the point mutants (not shown), which, together with the fact that they bound peptide ligand, confirmed that they were properly folded.

Peptide Ligands. For ITC binding experiments, peptides KQTSV and YKQTSV (GL Biochem, Shanghai, China) corresponding to the last five or six residues of CRIPT were used. A dansylated version of the longer peptide, **D**-YKQTSV, was used in stopped-flow experiments. The numbering of the peptide ligand is as in Figure 1, with the C-terminal residue numbered 0 and subsequent residues −1, −2, etc., toward the N-terminus. For the NMR measurements, a longer version of the C-terminus of CRIPT[19] was expressed as a doubly labeled [^{15}N,^{13}C]lipoyl fusion protein in *E. coli*. The lipoyl−peptide fusion protein was loaded onto a nickel column, washed with 50 mM Tris-HCl (pH 8.5) and 400 mM NaCl, and subsequently eluted with 250 mM imidazole (pH 7.9). Fractions containing the lipoyl−peptide fusion protein were then pooled, filtered with a 0.2 μm filter, and loaded onto a Q-column equilibrated with 50 mM Tris-HCl (pH 8.5). The pure lipoyl−peptide fusion protein was eluted by a gradient from 0 to 500 mM NaCl in 50 mM Tris-HCl (pH 8.5). The peptide was cleaved from the fusion protein with thrombin and then purified by reversed phase high-performance liquid chromatography on a C18 column, lyophilized, and stored at −20 °C. The peptide contained two extra residues at the N-terminus, GS, from the thrombin cleavage site, thus resulting in the GSKNYKQTSV peptide. The identity was confirmed by

MALDI-TOF mass spectrometry. Prior to NMR experiments, the peptide was dissolved in the appropriate buffer and its concentration was determined by UV absorbance using a calculated extinction coefficient of 1490 cm^{-1} M^{-1}.

NMR Titrations. Titration experiments were performed on a Varian INOVA 600 MHz spectrometer equipped with a cryogenically cooled probe, at 283 and 277 K. Peptide samples were dissolved in 50 mM potassium phosphate (pH 7.5) and 10% D_2O, and $^1H-^{15}N$ HSQC spectra of the peptide (290 or 150 μM) were recorded at an increasing concentration of unlabeled PDZ3 (0, 260, 270, 310, and 370 μM) or unlabeled PDZ3Δα3 (0, 520, 820, and 940 μM). For backbone resonance assignments, ^{15}N NOESY-HSQC, ^{15}N TOCSY-HSQC, HNCACB, CBCA(CO)NH, HN(CA)CO, and HNCO spectra were recorded for the bound and unbound peptide. Aliphatic side chain resonance assignments were obtained using HCCH-TOCSY and ^{13}C NOESY-HSQC experiments. The aromatic side chain of Tyr_{-5} was assigned using ^{13}C-edited NOESY spectra optimized for the aromatic resonances. ^{13}C-edited NOESY experiments were used to detect inter- and intramolecular nuclear Overhauser enhancements (NOEs). Data processing and analysis were done with NMRpipe[20] and Sparky (Goddard, T. D., and Kneller, D. G., SPARKY 3, University of California, San Francisco, CA), respectively.

Stopped-Flow Experiments. Pre-equilibrium ligand binding experiments were performed on an upgraded SX-17 MV stopped-flow spectrometer (Applied photophysics, Leatherhead, U.K.). For k_{on} measurements, the concentration of protein (PDZ3, PDZ3Δα3, and point mutants Y397E, R399A, and F400A) was kept constant at 3 μM and the concentration of the **D**-YKQTSV peptide was varied. The experiments were performed at 10 °C in 50 mM potassium phosphate (pH 7.5). Excitation of Trp_{337} was conducted at 280 nm, while the emission was recorded using a 330 nm band-pass filter. Traces obtained from pre-equilibrium ligand binding were fit to a single-exponential function (eq 1).

$$A = \Delta A_{EQ}(1 - e^{-k_{obs}t}) + C \quad (1)$$

where A is the change in florescence over time t and k_{obs} is the observed rate constant. The k_{obs} values were plotted against the peptide concentration and fit to eq 2.

$$k_{obs} = [k_{on}^2(n - [A]_0)^2 + k_{off}^2 + 2k_{on}k_{off}(n + [A]_0)]^{0.5} \quad (2)$$

where k_{on} is the association or on-rate constant and k_{off} is the dissociation or off-rate constant. $[A]_0$ and n are the total concentrations of peptide and protein (held constant at 3 μM), respectively.[21]

The off-rate constant was measured separately for PDZ3, PDZ3Δα3, and point mutants Y397E, R399A, and F400A. For these experiments, protein (3 μM) was preincubated with the **D**-YKQTSV peptide (3 μM). The complex was dissociated via the addition of the unlabeled YKQTSV peptide, and the resulting traces were fit to eq 1. k_{obs} values thus obtained were plotted versus the concentration of unlabeled peptide and fit to eq 3.

$$k_{obs} = k_{off} + k_{on}'[K_D/(K_D + n)] \quad (3)$$

where n is the concentration of the unlabeled peptide, K_D is the equilibrium dissociation constant for the unlabeled peptide and the PDZ domain, and k_{on}' is the apparent (first-order) on-rate constant for the PDZ domain and the dansylated peptide at the particular peptide concentration used in the experiment. At high n values, the observed rate constant k_{obs} approaches the dissociation rate constant k_{off}, which is well determined in the curve fitting.

Equation 4 was used to determine the change in binding free energy of the PDZ–peptide interaction upon mutation, $\Delta\Delta G$ (Table 1).

$$\Delta\Delta G = -RT \times \ln[(k_{off}^{WT}k_{on}^{mut})/(k_{off}^{mut}k_{on}^{WT})] \quad (4)$$

where R is the gas constant and T is the temperature in kelvin.

Table 1. Binding Constants for the Interaction between Dansylated Peptide D-YKQTSV and Wild-Type and Mutant PDZ3[a]

PDZ	k_{off} (s^{-1})	k_{on} ($\mu M\ s^{-1}$)	K_D (k_{off}/k_{on}) (μM)	$\Delta\Delta G$ (kcal/mol)
PDZ3	1.6 ± 0.20	11 ± 0.20	0.15 ± 0.02	
PDZ3Δα3	150 ± 40	13 ± 3	11 ± 4	2.4 ± 0.4
Y397E	40 ± 2	8.0 ± 0.3	5 ± 0.3	2.0 ± 0.15
R399A	6.0 ± 0.3	10 ± 1	0.6 ± 0.07	0.8 ± 0.2
F400A	50 ± 1.0	19 ± 3	2.7 ± 0.4	1.6 ± 0.2

[a] k_{on} and k_{off} values were obtained from fitting eqs 2 and 3, respectively, to the k_{obs} values from pre-equilibrium ligand binding stopped-flow measurements. Errors in k_{on} and k_{off} are fitting errors, while the other errors are propagated fitting errors.

Competition Ligand Binding Experiments. To estimate K_D values of YKQTSV and KQTSV, competition ligand binding experiments were performed in the SX-17 MV stopped-flow spectrometer in 50 mM potassium phosphate (pH 7.5) at 10 °C. For the measurements, a complex formed by preincubating 2 or 3 μM protein (either PDZ3 or PDZ3Δα3) with 4 or 6 μM **D**-YKQTSV peptide, respectively, was dissociated with different concentrations of the nondansylated peptide (either YKQTSV or KQTSV). The resulting change in the dansyl fluorescence was monitored and plotted versus peptide concentration. Excitation was conducted at 280 nm (excitation of Trp_{337}), while the emission was recorded using a 330 nm band-pass filter in the stopped flow. Data from the competition ligand binding were fit to eq 5.[18]

$$F = \{(K_{D1} + K_{D1}[L_2]/K_{D2} + [P]_t + [L_1]_t)/2 - [(K_{D1} + K_{D1}[L_2]/K_{D2} + [P]_t + [L_1]_t)^2/4 - [P]_t[L_1]_t]^{0.5}\} \times B + C \quad (5)$$

where F is the observed fluorescence signal at equilibrium and K_{D1} and K_{D2} are the dissociation constants of L_1 and L_2, respectively. $[L_1]_t$ is the total concentration of the **D**-YKQTSV peptide that was held constant at 4 or 6 μM, while $[L_2]$ is either the YKQTSV or KQTSV peptide concentration that was varied between 0–100 and 0–470 μM. $[P]_t$ is the total concentration of either PDZ3 or PDZ3Δα3 held constant at 2 or 3 μM. B is the total fluorescence change, and C is the end point. The K_{D1} value for the dansylated peptide for PDZ3 and PDZ3Δα3 was calculated from the ratio of k_{off} to k_{on} (Table 1) and used in eq 5. The K_{D2} values for YKQTSV and KQTSV are reported in the legend of Figure 6.

Isothermal Titration Calorimetry (ITC) Experiments. ITC experiments were conducted in an ITC200 microcalorimeter with a 200 μL cell volume (GE Healthcare). The PDZ solution dialyzed in 50 mM potassium phosphate (pH 7.5) was placed in the sample cell. A peptide stock was

dx.doi.org/10.1021/bi300792h | Biochemistry 2012, 51, 8971–8979

Table 2. ITC Binding Data for PDZ−Peptide Interactions

	YKQTSV				KQTSV			
PDZ	ΔH (kcal/mol)	$-T\Delta S$ (kcal/mol)	K_D (μM)	n	ΔH (kcal/mol)	$-T\Delta S$ (kcal/mol)	K_D (μM)	n
PDZ3	−10 ± 1	1.9 ± 0.2	1 ± 0.1	0.8 ± 0.1	−4.0 ± 0.1	−3.8 ± 0.4	2.0 ± 0.3	1 ± 0.1
PDZ3Δα3	−3.4 ± 0.6	−3.7 ± 0.6	6 ± 0.2	0.9 ± 0.1	nd[a]	nd[a]	nd[a]	nd[a]

[a]Not detectable.

prepared in 50 mM potassium phosphate (pH 7.5), and aliquots of 1.5 μL (0.12−0.24 mM for YKQTSV and 0.24−1 mM for KQTSV) were injected into the cell containing either a PDZ3 (8−13 μM) or PDZ3Δα3 (15 μM) protein solution at 25 °C. Once the titration was completed, the raw data were then fit using the "one-binding site model" of the MicroCal version of ORIGIN. Experiments were performed in duplicate or triplicate (for the wild-type or mutant proteins, respectively). As a control, the heat exchange of peptide dilution into buffer has been measured and taken into account in data analysis. In our experiments, although the baseline is slightly noisy, as expected for a highly sensitive instrument, the reproducibility is very good as shown by the small experimental errors listed in Table 2. Therefore, although the c value is slightly low,[22] in particular for the mutant, the curve is not too shallow and is completed in a single experiment. The heat of binding (ΔH), the stoichiometry (n), and the dissociation constant (K_D) were then calculated from plots of the heat evolved per mole of ligand injected versus the molar ratio of ligand to protein using the software provided by the manufacturer.

RESULTS

First, we performed NMR experiments to see which peptide ligand residues interact with the protein. Next, to determine the contribution of the binding free energy of helix α3 to formation of the PDZ3−peptide complex, we performed equilibrium and pre-equilibrium binding experiments with peptide ligand and wild-type or mutant PDZ3.

At Least Eight Peptide Residues Interact with PDZ3. To determine which residues in the peptide likely interact with PDZ3, we monitored chemical shift changes in ^{1}H−^{15}N HSQC and ^{1}H−^{13}C HSQC spectra of a fully labeled peptide (290 or 150 μM) with saturating amounts of PDZ3 (520 μM) and a variant in which helix α3 was removed, PDZ3Δα3 (940 μM), respectively. The chemical shifts were assigned to the free and bound peptide. In the free peptide, eight of the resonances were observed at 277 K and six of the resonances were observed at 283 K (Figure 2). The discrepancy is likely due to a higher rate of amide proton exchange with solvent at the higher temperature. In the bound form, the backbone ^{1}H−^{15}N resonances of eight residues (Figure 2A) and the ^{1}H−^{13}C resonances of the side chains of all residues (data not shown) were observed and assigned with the exception of CB of Thr$_{-2}$ for the peptide bound to PDZ3Δα3. ^{1}H−^{13}C and ^{1}H−^{15}N combined chemical shift perturbations upon binding (CSP) were observed throughout the peptide except for Gly$_{-9}$ both for the backbone and for side chain residues, showing that most of the peptide experiences significant changes in the environment upon interaction with the protein (Figure 3). However, our data cannot be used to conclusively state that all residues of the peptide are interacting with the PDZ domain because CSPs for residues that do not interact can be the result of conformational changes in the peptide itself due to interaction with PDZ3 in another part of the peptide. It is, however, noteworthy that the

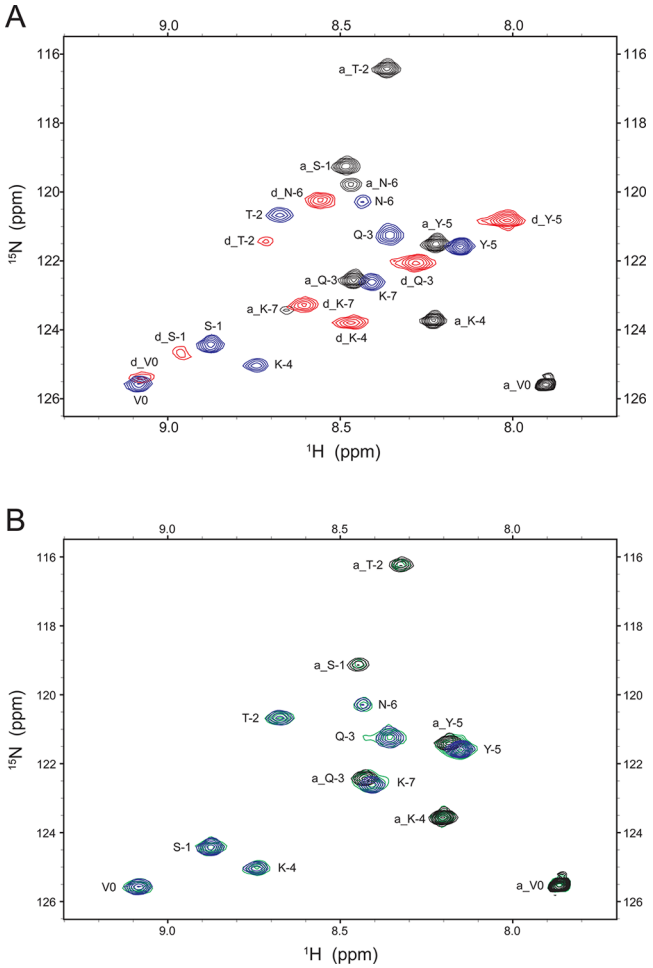

Figure 2. ^{1}H−^{15}N HSQC spectra of the GSKNYKQTSV peptide in complex with PDZ3 and PDZ3Δα3. (A) Data for the apo-peptide are colored black, data for the peptide in complex with PDZ3 blue (>99% saturation), and data for the peptide in complex with PDZ3Δα3 red (>98% saturation). The nomenclature of the residues is as follows: a_V0 is the C-terminal valine in the apo-peptide, d_V0 is the C-terminal valine in the peptide in complex with PDZ3Δα3, and V0 is the C-terminal valine in the peptide in complex with PDZ3. (B) HSQC spectrum of the peptide at 0% (black), 89% (green), and >99% (blue) saturation of PDZ3. Note that the apo-peptide spectrum in panel A was recorded at 277 K whereas the one in panel B was recorded at 283 K, hence the slightly different appearance. As expected, more peaks are present at the lower temperature.

CSPs, for residues Lys$_{-7}$ to Gln$_{-3}$, differ significantly for binding to PDZ3 and PDZ3Δα3. It is therefore tempting to speculate that these residues interact differently with the two forms of the PDZ domain and that helix α3 is involved in the binding to wild-type PDZ3.

In the crystal structure [Protein Data Bank (PDB) entry 1BE9] of PDZ3 in complex with the TKNYKQTSV peptide, the motif closest to the N-terminus of the peptide is α3, which

dx.doi.org/10.1021/bi300792h | Biochemistry 2012, 51, 8971−8979

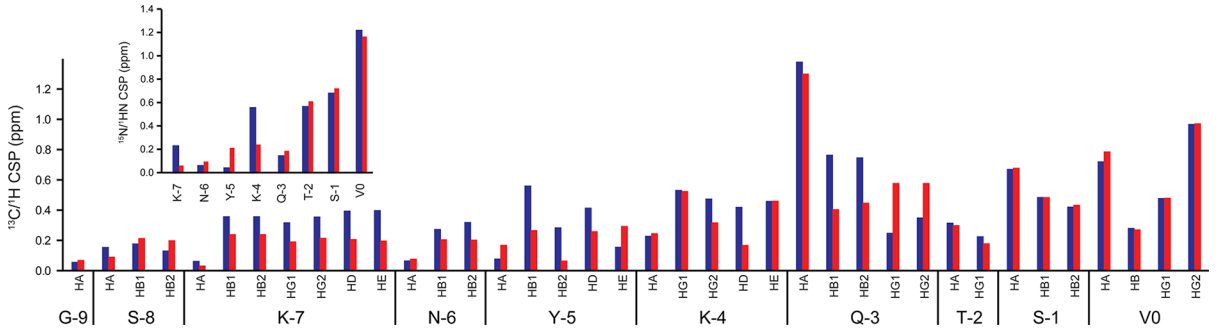

Figure 3. Chemical shift differences upon peptide binding. $^{13}C/^{1}H$ chemical shift perturbation for peptide side chains upon binding to either PDZ3 (blue) or PDZ3Δα3 (red). The inset shows the $^{15}N/^{1}H$ chemical shift difference of the backbone amides upon binding to PDZ3 (blue) or PDZ3Δα3 (red). The ^{13}C and ^{15}N chemical shift perturbations were calculated as $[\Delta\phi_H^2 + (\Delta\phi_C \times 0.25)^2]^{0.5}$ and $[\Delta\phi_H^2 + (\Delta\phi_N \times 0.1)^2]^{0.5}$, respectively. Assignments of the HB1 and HB2 type do no indicate stereospecific assignments but are merely a way of labeling protons with distinct chemical shifts that are bound to the same carbon.

is 5 Å from peptide residue Gln_{-3}. No electron density was observed for the TKNYK residues at the N-terminus of the peptide.[13] However, in the crystal structure of PDZ3 in complex with another peptide, KKETPV (PDB entry 1TP3), Lys_{-4} is ∼4 Å from the side chain His_{372}. To see if the combined chemical shifts observed were due to direct interaction with the protein or if they were merely due to titration perturbation (upon addition of PDZ3), we performed NOESY-HSQC and HCCH-TOCSY experiments with the peptide in complex with PDZ3 and PDZ3Δα3, respectively. By identifying peaks present in the NOESY-HSQC spectra but absent in the HCCH-TOCSY spectra, we observed several NOEs (Figure 4) between the respective protein and the peptide backbone and side chain residues from position 0 to −6.

To further rule out the possibility that NOEs identified as intermolecular were in fact not intramolecular, we carefully checked the NOESY spectra for candidates with matching chemical shifts and confirmed that corresponding peaks were absent (Figure 4, panel V). Importantly, the intermolecular NOEs obtained with wild-type PDZ3 were different from those with PDZ3Δα3, demonstrating that the peptide forms distinct transient interactions in the two cases and suggesting that helix α3 may interact directly with the peptide ligand. To prove the latter hypothesis, we would, however, need to perform the reverse experiment, i.e., to use isotopically labeled PDZ domain and determine which of its nuclei interact with the peptide in NOESY experiments. Admittedly, the sensitivity is poor in all NOESY experiments because of the low concentration and low temperature, especially experiments involving the peptide bound to PDZ3Δα3. Thus, we likely observed too few rather than too many intermolecular contacts.

In a previous study in which the influence of binding of helix α3 of PDZ3 was investigated, the authors concluded that α3 modulates PDZ3 binding through entropy-driven dynamic allostery rather than direct interactions.[14] They did not detect any significant chemical shift changes for peptide residues other than residues −3 to 0 using natural abundance $^{1}H-^{13}C$ HSQC spectra recorded at 298 K (Figure 6 of ref 14). Furthermore, the concentration dependence of the chemical shift changes of these nuclei in these residues suggests exchange in the fast regime. However, in the work presented here, we used a fully ^{13}C- and ^{15}N-labeled peptide and a saturating concentration of protein and recorded our data at 277 and 283 K using a slightly different form of the peptide. As noted during our NMR

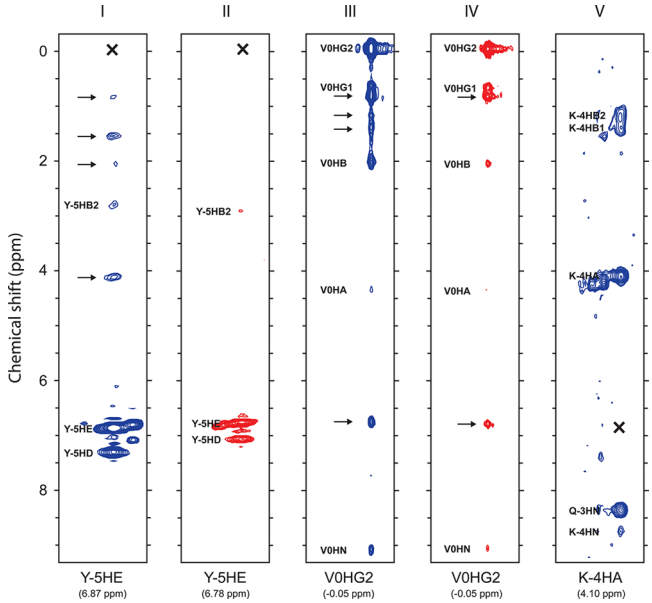

Figure 4. NOESY-HSQC spectra of Lys_{-4} and Tyr_{-5}. Intra- and intermolecular NOEs involving HE of Tyr_{-5}(I and II) and HG2 of Val_0 (III and IV) of the peptide (290 or 150 μM) saturated with PDZ3 (I and III) or PDZ3Δα3 (II and IV), respectively, as well as HA of Lys_{-4} of the peptide in complex with PDZ3 (V). For the sake of clarity, the peaks in the panels showing the peptide in complex with PDZ3 are colored blue and those for PDZ3Δα3 are colored red. Assignments of intramolecular NOEs are shown, and unassigned intermolecular NOEs to the PDZ domain are highlighted with an arrow. The absence of putative intramolecular NOEs is indicated with a cross. Note the disappearance of certain NOEs when helix α3 is deleted (I vs II and III vs IV).

titrations, at 89% saturation, most residues were in slow exchange and appeared as double peaks (14 in total) in the HSQC spectrum (Figure 2B). Complete perturbation was observed only at 99% saturation, which could explain the discrepancy regarding the number of peptide residues making direct contact with the protein (the previous data were for a 15% molar ratio) (Figure 2B). In addition, Petit et al. used a peptide with a slightly different sequence at the N-terminus and N-acetylation, which was previously shown to reduce the affinity for peptide−PDZ3 interactions.[15]

Deletion of Helix α3 and Tyr_{-5} Induces a Favorable Entropy of Binding. To analyze the thermodynamics of the

dx.doi.org/10.1021/bi300792h | Biochemistry 2012, 51, 8971−8979

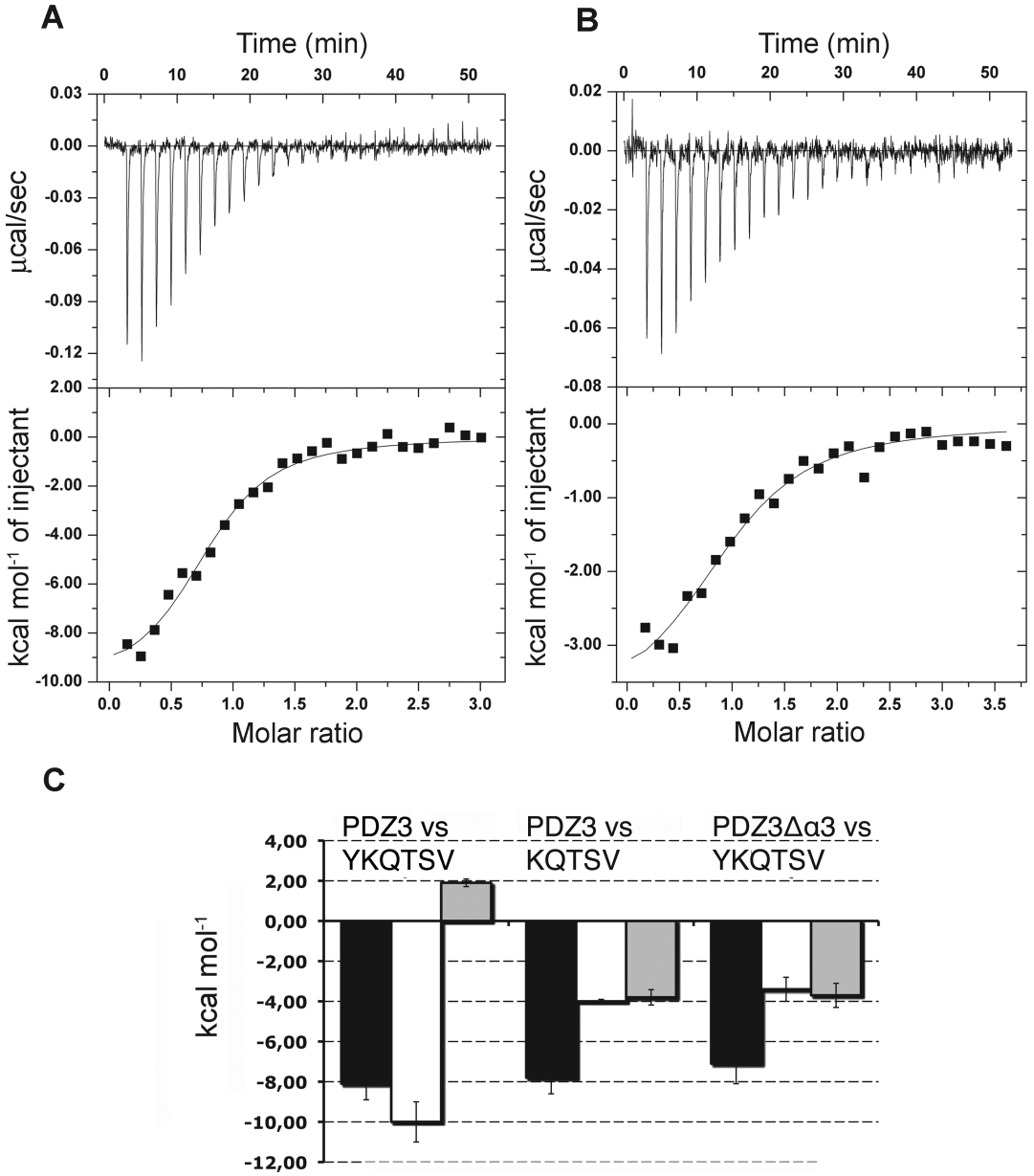

Figure 5. Thermodynamics of the PDZ−peptide interaction. Isothermal titration calorimetric experiments with (A) PDZ3 and YKQTSV and (B) PDZ3 and KQTSV. The top panels show the raw ITC data and the bottom panels integrated peak areas (■) and fits with the one-binding site model of ORIGIN provided by MicroCal (—). The concentrations used in these experiments were (A) 8 μM PDZ3 and 0.12 mM YKQTSV and (B) 13 μM PDZ3 and 0.18 mM KQTSV. (C) Plot of ΔG (black bars), ΔH (white bars), and $-T\Delta S$ (gray bars) derived from the data and also reported in Table 2.

PDZ−peptide interaction and in particular the role of Tyr_{-5}, because this peptide residue may interact with α3, we performed ITC experiments with both PDZ3 and PDZ3$\Delta\alpha$3 with two peptides, KQTSV and YKQTSV (Figure 5). The fitted parameters from three of these four separate experiments are summarized in Table 2. PDZ3 interacts with the YKQTSV peptide with a highly favorable enthalpy (ΔH = −10 kcal/mol) and slightly unfavorable entropy ($-T\Delta S$ = 1.9 kcal/mol). Upon deletion of Tyr_{-5} from the peptide, the enthalpy of binding was reduced to −4 kcal/mol, and this was associated with a favorable entropic term ($-T\Delta S$ = −3.8 kcal/mol). This result is similar to that of the case in which helix α3 was deleted from PDZ3 (ΔH = −3.4 kcal/mol, and $-T\Delta S$ = −3.7 kcal/mol). Unfortunately, we did not see any change in heat when both helix α3 and Tyr_{-5} were deleted (data not shown). The likely reason for this is a low affinity between PDZ3$\Delta\alpha$3 and KQTSV, rather than a low enthalpic term, or possibly a combination of the two. Nonetheless, the short peptide was found to bind PDZ3$\Delta\alpha$3 in a competition assay (Figure 6). We attempted to directly demonstrate an interaction between helix α3 and Tyr_{-5} through a double mutant cycle (Figure 6), but the error in K_D for the interaction between PDZ3$\Delta\alpha$3 and KQTSV was too large, because of the low affinity, which precluded a reliable quantitative analysis of the coupling energy.

Single-Point Mutants in Helix α3 Destabilize the PDZ3−Peptide Complex. The results thus far suggested that residues Val_0 to Lys_{-7} in the peptide are involved in complex formation and that helix α3 in PDZ3 increases the affinity. We therefore tested which individual side chain residues in helix α3 contribute to binary complex formation, by making the

dx.doi.org/10.1021/bi300792h | *Biochemistry* 2012, 51, 8971−8979

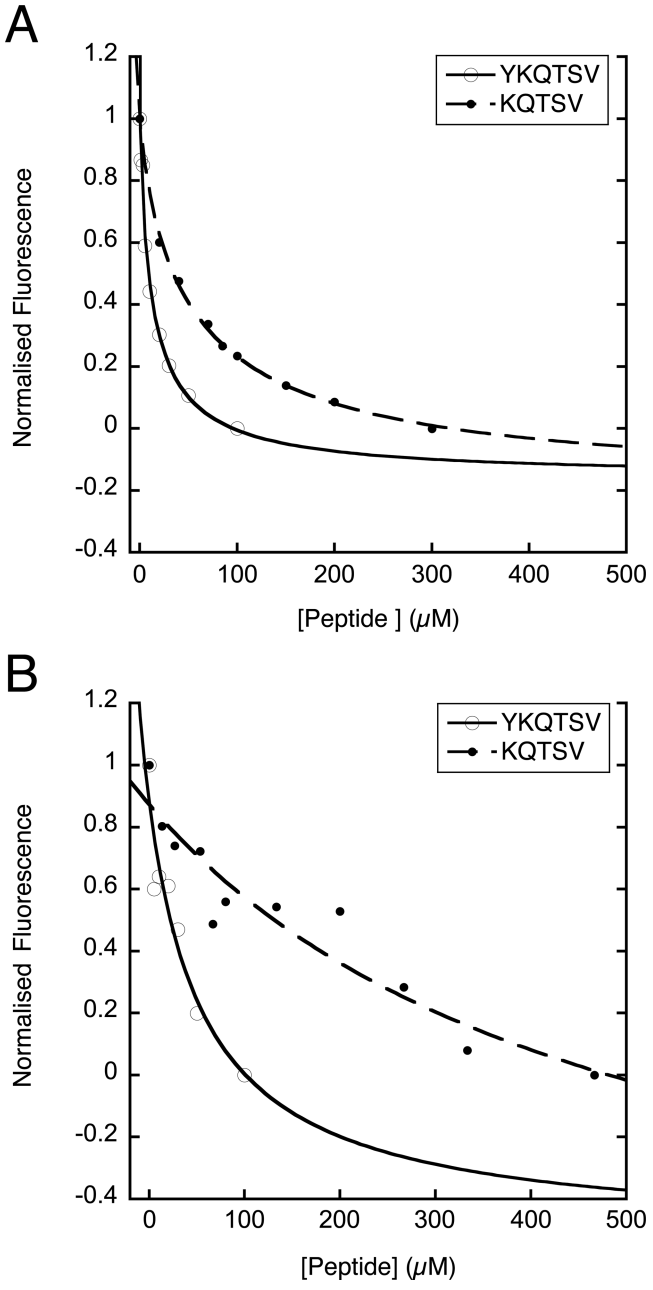

Figure 6. Equilibrium displacement experiments. A complex of **D**-YKQTSV (3 μM) and either (A) PDZ3 or (B) PDZ3Δα3 was dissociated with YKQTSV or KQTSV in separate experiments. If the affinity for **D**-YKQTSV (K_{D1}) is known, the affinity for the unlabeled peptides (K_{D2}) can be estimated using eq 5 as described in Materials and Methods. K_{D2} values were 1.0 ± 0.3 and 4.3 ± 0.3 μM for PDZ3 with YKQTSV and KQTSV, respectively. However, the low affinity of PDZ3Δα3 for both YKQTSV (43 ± 36 μM) and in particular KQTSV (360 ± 320 μM) yielded an error in the analysis that is on the same order of magnitude as the value, precluding a quantitative analysis of the interaction and the calculation of a reliable coupling free energy between helix α3 and Tyr$_{-5}$. These experiments were performed in the stopped-flow fluorimeter, and normalized kinetic end points are plotted on the *y*-axes.

following point mutants in helix α3: Y397E (a phosphorylation mimic[23]) and deletion mutants R399A and F400A. The side chains of these residues point toward the peptide binding groove and may interact with a bound peptide. The point mutants as well as the wild type and PDZ3Δα3 were subjected to pre-steady-state binding experiments (Figure 7 and Table 1). The k_{off} values for the interaction between the mutants, Y397E, R399A, and F400A, and the dansylated peptide, **D**-YKQTSV, increased by factors of 26, 4, and 30, respectively, showing that these residues contribute significantly to the binding of the dansylated peptide ligand (Table 1). It is therefore likely that these side chains will contribute to binding of natural ligands, either through direct and transient interactions or indirectly by stabilizing helix α3.[24]

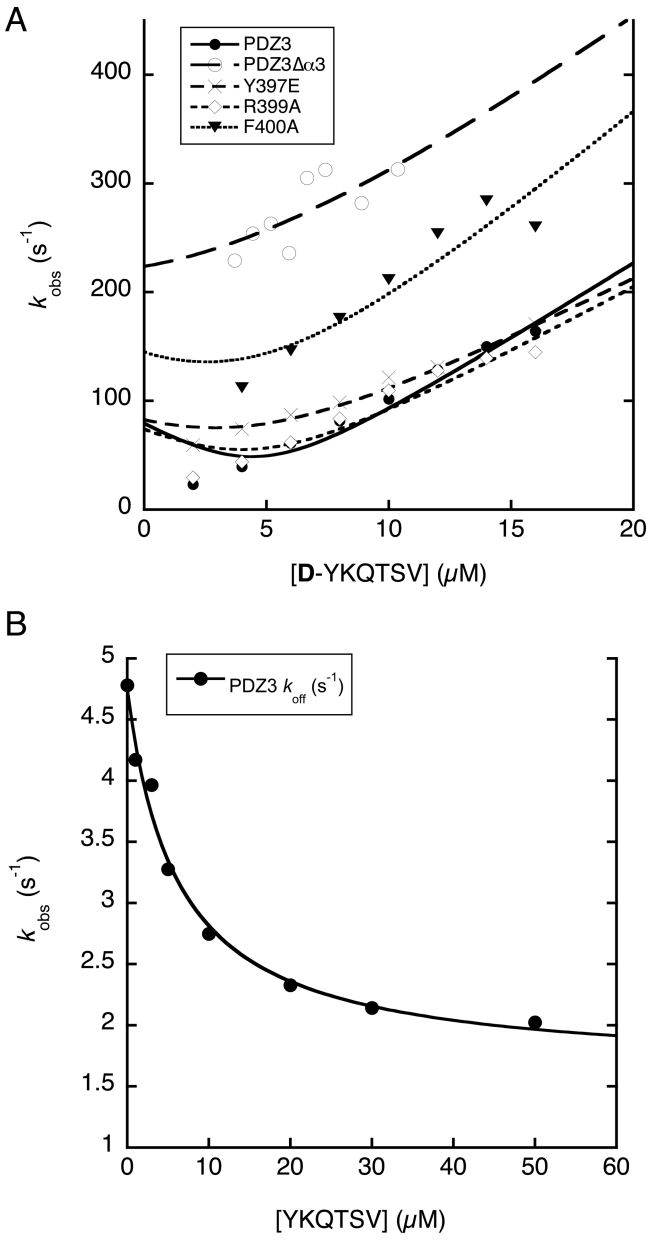

Figure 7. Pre-equilibrium binding data for PDZ3 and mutants. (A) Observed rate constants for the interaction of PDZ and peptide plotted vs the increasing concentration of the dansylated peptide **D**-YKQTSV. (B) Observed rate constants for the displacement of the PDZ3–**D**-YKQTSV complex plotted vs the increasing YKQTSV concentration. The rate constant at the high concentration of unlabeled peptide is equal to the off-rate constant in the interaction of PDZ3 with **D**-YKQTSV.

dx.doi.org/10.1021/bi300792h | *Biochemistry* 2012, 51, 8971–8979

DISCUSSION

The binding energy in the interaction between PDZ domains and their ligands comes mainly from hydrophobic interactions and hydrogen bonds in the canonical binding groove,[13,15] but because the PDZ domain ligand is often very flexible, it can wrap around the surface of the PDZ domain to make additional favorable interactions outside of the canonical binding groove. This binding groove is typically occupied by only four ligand residues, as defined by hydrogen bonds between backbones of the peptide and the second β-strand of the PDZ domain (see Figure 1).

The contribution to the binding free energy of the PDZ3−peptide interaction by residues in the peptide ligand other than the four at the C-terminus was thoroughly investigated by Saro et al. using ITC.[15] Their results showed that residues 0 to −5 (see Figure 1) are important for PDZ3−peptide affinity, while further addition had a minimal effect on the thermodynamics of binding. For example, the presence of Tyr_{-5} was found to increase the affinity 10-fold at pH 6.0. Our data further confirm the importance of Tyr_{-5} in the PDZ3−peptide interaction. However, we also showed that residues −4 and −7 show changes in chemical shifts upon binding, although the net energetic contribution of residues −6 and −7 to the affinity is small. Nonetheless, it is clear from our data that the N-terminal regions of long C-termini of PDZ ligands may explore a large binding surface outside of the peptide-binding groove.

All residues in the vicinity of the binding groove may afford such an extra binding surface, but helix α3 in PDZ3 is particularly interesting in this respect because it is a so-called noncanonical structural element[25,26] found in only some PDZ domains and for example not in the other two PDZ domains of PSD-95. Our ITC data suggest that helix α3 in PDZ3 contributes a binding free energy for the CRIPT ligand of approximately 1.1 kcal/mol, and the fluorescence-based binding data give free energies of 2.4 kcal/mol (dansylated peptide) and 2.2 kcal/mol (Figure 6, large error), in qualitative agreement with published data for a longer peptide (1.8 kcal/mol).[14] Moreover, we detected intermolecular NOEs between PDZ3 and Tyr_{-5} of the peptide. The absence of these intermolecular NOEs in experiments with labeled peptide and PDZ3Δα3 indicates that helix α3 may in fact be involved in direct short-lived interactions with peptide ligand side chains, although it remains to be proven.

The point mutations in helix α3 further demonstrate the importance of this helix. A recent computational study by Mostarda et al.[24] shed light on the destabilizing effects of the mutations. They found by molecular dynamics simulations that Tyr_{397} and Phe_{400} make stabilizing hydrophobic interactions with each other and with residues in PDZ3, Arg_{399} makes a transient salt bridge with Glu_{334}, which in turn stabilizes the β2−β3 loop, and Glu_{401} interacts with Lys_{355}. Thus, mutation of these residues (as well as the complete removal of helix α3) might influence binding indirectly by destabilization of a preorganized binding site for the peptide. They also observed transient salt bridges between Glu_{331} and Asp_{332} in PDZ3 and Lys_{-4} and Lys_{-7} in the CRIPT peptide, along with unstable hydrophobic contacts between the peptide and helix α3. The E331A mutation indeed results in a decreased k_{on} and an increased k_{off}.[9] Thus, simulation[24] and experiment conspire to reveal a protein−ligand interaction for PDZ3 governed by (i) stable interactions ($t_{1/2} \sim 1/k_{off}$) in the canonical binding site,[9,13,15] (ii) transient ($t_{1/2} \ll 1/k_{off}$) but direct interactions outside of this binding site involving, for example, Glu_{331} and most likely portions of α3, and (iii) long-range interactions.[9,14,17]

The additional C-terminal extension is not unique for PDZ3.[25,26] In MAGI PDZ1, for example, an extended C-terminal loop makes direct interactions with Arg_{-4}, Arg_{-5}, and Thr_{-6} of the peptide ligand and mutation in this C-terminal loop decreases the binding affinity drastically.[27] Thus, from previous work[11,12,14,24,27] together with the data presented here, we conclude that some PDZ domains contain certain structural elements at their C-termini, which have a direct effect on binding affinity.

An appealing model is one in which such binding surfaces in PDZ domains increase not only the affinity for the ligand but also the specificity. For example, the peptide residues at positions −6 and −7 of CRIPT appear not to have a net positive energetic effect on the binding of PDZ3,[15] but they might well have a negative effect on binding to other PDZ domains. In the case of PDZ3 from PSD-95, helix α3 is likely to provide part of an extended binding surface and in this way increase the specificity toward its natural ligand, CRIPT.

AUTHOR INFORMATION

Corresponding Author

*P.L.: e-mail, patlu@ifm.liu.se; phone, +46-13-286 650. P.J.: e-mail, per.jemth@imbim.uu.se; phone, +46-18-471 4557.

Funding

This work was supported by the Swedish Research Council (to P.J. and P.L.), Lars Hiertas Minne and the Royal Swedish society (to C.N.C.), the Italian Ministero dell'Istruzione dell'Università e della Ricerca, Progetto di Interesse 'Invecchiamento' (to S.G.), the Ministero dell'Istruzione, Università e Ricerca of Italy (RBRN07BMCT_007) (to F.C.), (RBFR10LHD1_001) (to S.R.), and the Sapienza University of Rome (Italy) (to F.C.).

Notes

The authors declare no competing financial interest.

ABBREVIATIONS

ITC, isothermal titration calorimetry; PDZ, postsynaptic density protein-95/discs large/zonula occludens-1; PSD-95, postsynaptic density protein-95.

REFERENCES

(1) Nourry, C., Grant, S. G. N., and Borg, J.-P. (2003) PDZ Domain Proteins: Plug and Play! *Sci. STKE 2003*, re7.

(2) Kim, E., Niethammer, M., Rothschild, A., Jan, Y. N., and Sheng, M. (1995) Clustering of Shaker-type K^+ channels by interaction with a family of membrane-associated guanylate kinases. *Nature 378*, 85−88.

(3) Kornau, H. C., Schenker, L. T., Kennedy, M. B., and Seeburg, P. H. (1995) Domain interaction between NMDA receptor subunits and the postsynaptic density protein PSD-95. *Science 269*, 1737−1740.

(4) Niethammer, M., Kim, E., and Sheng, M. (1996) Interaction between the C terminus of NMDA receptor subunits and multiple members of the PSD-95 family of membrane-associated guanylate kinases. *J. Neurosci. 16*, 2157−2163.

(5) Jemth, P., and Gianni, S. (2007) PDZ domains: Folding and binding. *Biochemistry 46*, 8701−8708.

(6) Chi, C. N., Bach, A., Strømgaard, K., Gianni, S., and Jemth, P. (2012) Ligand binding by PDZ domains. *BioFactors*, DOI: 10.1002/biof.1031.

(7) Wiedemann, U., Boisguerin, P., Leben, R., Leitner, D., Krause, G., Moelling, K., Volkmer-Engert, R., and Oschkinat, H. (2004) Quantification of PDZ Domain Specificity, Prediction of Ligand

Affinity and Rational Design of Super-binding Peptides. *J. Mol. Biol. 343*, 703−718.
(8) te Velthuis, A. J. W., Sakalis, P. A., Fowler, D. A., and Bagowski, C. P. (2011) Genome-Wide Analysis of PDZ Domain Binding Reveals Inherent Functional Overlap within the PDZ Interaction Network. *PLoS One 6*, e16047.
(9) Gianni, S., Haq, S. R., Montemiglio, L. C., Jürgens, M. C., Engström, Å., Chi, C. N., Brunori, M., and Jemth, P. (2011) Sequence-specific Long Range Networks in PSD-95/Discs Large/ZO-1 (PDZ) Domains Tune Their Binding Selectivity. *J. Biol. Chem. 286*, 27167−27175.
(10) Fuentes, E. J., Der, C. J., and Lee, A. L. (2004) Ligand-dependent Dynamics and Intramolecular Signaling in a PDZ Domain. *J. Mol. Biol. 335*, 1105−1115.
(11) Nomme, J., Fanning, A. S., Caffrey, M., Lye, M. F., Anderson, J. M., and Lavie, A. (2011) The Src Homology 3 Domain Is Required for Junctional Adhesion Molecule Binding to the Third PDZ Domain of the Scaffolding Protein ZO-1. *J. Biol. Chem. 286*, 43352−43360.
(12) Pan, L., Chen, J., Yu, J., Yu, H., and Zhang, M. (2011) The Structure of the PDZ3-SH3-GuK Tandem of ZO-1 Protein Suggests a Supramodular Organization of the Membrane-associated Guanylate Kinase (MAGUK) Family Scaffold Protein Core. *J. Biol. Chem. 286*, 40069−40074.
(13) Doyle, D. A., Lee, A., Lewis, J., Kim, E., Sheng, M., and MacKinnon, R. (1996) Crystal structures of a complexed and peptide-free membrane protein-binding domain: Molecular basis of peptide recognition by PDZ. *Cell 85*, 1067−1076.
(14) Petit, C. M., Zhang, J., Sapienza, P. J., Fuentes, E. J., and Lee, A. L. (2009) Hidden dynamic allostery in a PDZ domain. *Proc. Natl. Acad. Sci. U.S.A. 106*, 18249−18254.
(15) Saro, D., Li, T., Rupasinghe, C., Paredes, A., Caspers, N., and Spaller, M. R. (2007) A Thermodynamic Ligand Binding Study of the Third PDZ Domain (PDZ3) from the Mammalian Neuronal Protein PSD-95. *Biochemistry 46*, 6340−6352.
(16) Gianni, S., Engström, Å., Larsson, M., Calosci, N., Malatesta, F., Eklund, L., Ngang, C. C., Travaglini-Allocatelli, C., and Jemth, P. (2005) The kinetics of PDZ domain-ligand interactions and implications for the binding mechanism. *J. Biol. Chem. 280*, 34805−34812.
(17) Chi, C. N., Elfström, L., Shi, Y., Snäll, T., Engström, Å., and Jemth, P. (2008) Reassessing a sparse energetic network within a single protein domain. *Proc. Natl. Acad. Sci. U.S.A. 105*, 4679−4684.
(18) Chi, C. N., Engström, Å., Gianni, S., Larsson, M., and Jemth, P. (2006) Two conserved residues govern the salt and pH dependencies of the binding reaction of a PDZ domain. *J. Biol. Chem. 281*, 36811−36818.
(19) Niethammer, M., Valtschanoff, J. G., Kapoor, T. M., Allison, D. W., Weinberg, T. M., Craig, A. M., and Sheng, M. (1998) CRIPT, a novel postsynaptic protein that binds to the third PDZ domain of PSD-95/SAP90. *Neuron 20*, 693−707.
(20) Delaglio, F., Grzesiek, S., Vuister, G. W., Zhu, G., Pfeifer, J., and Bax, A. (1995) NMRPipe: A multidimensional spectral processing system based on UNIX pipes. *J. Biomol. NMR 6*, 277−293.
(21) Malatesta, F. (2005) The study of bimolecular reactions under non-pseudo-first order conditions. *Biophys. Chem. 116*, 251−256.
(22) Wiseman, T., Williston, S., Brandts, J. F., and Lin, L. N. (1989) Rapid measurement of binding constants and heats of binding using a new titration calorimeter. *Anal. Biochem. 179*, 131−137.
(23) Zhang, J., Petit, C. M., King, D. S., and Lee, A. L. (2011) Phosphorylation of a PDZ Domain Extension Modulates Binding Affinity and Interdomain Interactions in Postsynaptic Density-95 (PSD-95) Protein, a Membrane-associated Guanylate Kinase (MAGUK). *J. Biol. Chem. 286*, 41776−41785.
(24) Mostarda, S., Gfeller, D., and Rao, F. (2012) Beyond the Binding Site: The Role of the $\beta2-\beta3$ Loop and Extra-Domain Structures in PDZ Domains. *PLoS Comput. Biol. 8*, e1002429.
(25) Wang, C., Pan, L., Chen, J., and Zhang, M. (2010) Extensions of PDZ domains as important structural and functional elements. *Protein Cell 1*, 737−751.
(26) Bhattacharya, S., Dai, Z., Li, J., Baxter, S., Callaway, D. J. E., Cowburn, D., and Bu, Z. (2010) A Conformational Switch in the Scaffolding Protein NHERF1 Controls Autoinhibition and Complex Formation. *J. Biol. Chem. 285*, 9981−9994.
(27) Charbonnier, S., Nominé, Y., Ramírez, J., Luck, K., Chapelle, A., Stote, R. H., Travé, G., Kieffer, B., and Atkinson, R. A. (2011) The Structural and Dynamic Response of MAGI-1 PDZ1 with Non-canonical Domain Boundaries to the Binding of Human Papillomavirus E6. *J. Mol. Biol. 406*, 745−763.